

Microstructure characterization of Al-alloy AW 5454 intended for ecological laser hybrid welding

Matjaž Balant, Rebeka Rudolf*

University of Maribor, Faculty of Mechanical Engineering, Slomškov Trg 15, 2000 Maribor, Slovenia

ARTICLE INFORMATION :

<https://doi.org/10.56801/MMD30>

Received: 05 June 2024

Accepted: 19 June 2024

Type of paper: Research paper



Copyright: © 2023 by the authors, under the terms and conditions of the Creative Commons Attribution (CC BY) license (<https://creativecommons-mons.org/licenses/by/4.0/>).

ABSTRACT

This article presents the microstructure characterization of Al-alloy AW 5454, which is intended for laser hybrid welding. In the first part, the procedure of laser hybrid welding is described and compared to other laser surface modification techniques. Subsequently, key methods of metallographic characterization and hardness measurements at selected locations of Al-alloy AW 5454 are presented, enabling a scientific evaluation of the obtained results. The goal of the research was to gain insight into the microstructure of Al-alloy AW 5454, which will, in the future, make it possible to determine the technological parameters of laser hybrid welding that have the greatest influence on the final microstructure and, consequently, on the properties of the weld.

Keywords: Al-alloys, laser treatment, characterization, microstructure, hardness.

1. Introduction

A review of the professional and scientific literature shows that until now very little research has been done in the field of laser welding of Al-alloys (Cavaliere, 2021; Kandavalli et al., 2021; Nayak, 2004). Laser technology uses the phenomenon of stimulated radiation (emission) and amplification of light radiation as an energy source. The characteristics of laser light are high intensity, correct intensity distribution along the beam cross-section, low divergence, coherence, and characteristic wavelength (Renk, 2012). With laser surface modification, it is possible to achieve a combination of material properties that individual materials do not have. Laser surface modification can be roughly divided into two groups of procedures: (Saklakoglu et al., 2014; Trdan, U; Ocaña, J L; Grum, 2011): (i) laser surface modification processes with direct interaction of the laser with the Al-alloy are known as LSM (laser surface melting process)(Biswas, 2014) and (ii) procedures with indirect laser interaction with Al-alloy (shock waves, cavitation hardening). In the first group of procedures, laser beams locally heat the material's surface to a very high temperature, and have an effect up to a depth of 10-100 mm. Laser beams can heat, melt or vaporize matter, or create plasma depending on the energy input.

The pulse duration can be controlled and can be 1 ns or less. Subsequent cooling of the material leads to the re-hardening of the surface into the resulting fine-grained microstructure, where perfect

stacking is usually formed between the modified surface and the substrate. In some cases, cooling is so rapid that a glassy phase forms. In this process, the surface of the workpiece is prepared by first coating it with a suitable metal, alloy, or powder (Figure 1).

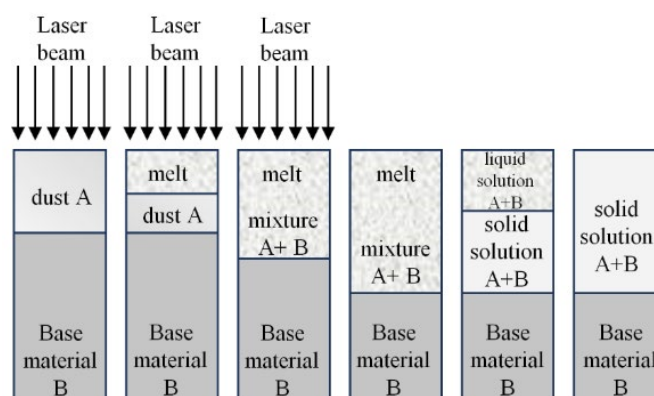


Fig. 1. Laser alloying of components A and B.

The resulting coating is heated by a laser beam, which causes it to melt together with the substrate to form a homogeneous melt, which is then cooled. The most important process variables in laser processing are energy input and pulse duration. For established techniques such as cutting, drilling, and welding there is an energy input of 1 MW/cm², and

* Corresponding author.

E-mail address: rebeka.rudolf@um.si (R. Rudolf).

pulses last up to 1 ms (Zupanič and Anžel, 2007). However, shock waves require an energy intake of up to 100 MW/cm² and pulse durations of up to 1 ns to harden metals.

Short pulses enable rapid cooling and the formation of metastable phases.

Laser surface modification techniques are (Watkins, McMahon, in Steen, 1997): (i) Laser remelting of the surface (Fribourg et al., 2011; Nayak, 2004; Tsagkarakis et al., 2003), (ii) Laser surface cladding (Cavaliere 2021; Chen et al., 2023; Liu et al., 2024; Nayak, 2004; Sui et al., 2023; Jin, Lu, and Tang, 2023; Zhao et al., 2023) - mixing occurs only at the cladding/substrate junction or above the junction, the composition and properties of the cladding materials are preserved, and (iii) laser alloying of the surface (Zupanič and Anžel, 2007). In the last process, significant mixing of the coating with the substrate is carried out to form an alloyed surface layer with new phases and compositions. The alloy layer is generally much thinner than the plating layer.

In processes with indirect laser interaction of the laser with the Al-alloy, laser impact treatment is very often used laser shock processing (LSP) (Abeens et al., 2019; He et al., 2021; Lu, Huang, and Zhong, 2012; Luo et al., 2024), where the key is to achieve the desired amount of residual stresses and improve the corrosion resistance of the workpiece (Trdan, U; Ocaña, J L; Grum, 2011; Saklakoglu et al., 2014). LSP is based on the generation of plasma at the moment of laser light interaction with the sample, which causes shock waves and elasto-plastically moves the atomic planes in the material.

The welding and alloying processes described above have the disadvantage that, as shown in Figure 1, they use pre-prepared particles/powders which, due to their properties, have their own shape and size (for example single-wall carbon nanotubes (SWCNTs) and multi-walled carbon nanotubes (MWNT))(Dai, 2002) controversial due to the impact on ecology (non-biodegradable) and the aspect of toxicity for humans and animals (Eatemadi et al., 2014; Simon, Flahaut, and Golzio, 2019). In laser hybrid welding, additional material is used in the form of wire, which is supplied directly to the welding site and is not objectionable in terms of the size of the residues and harmfulness/toxicity. Scraps are easily recycled, as Al-alloys are highly recyclable (Raabe et al., 2022).

In the framework of this study, the microstructure of Al alloy AW 5454 and its influence on the formation of potential cracks in the weld after the laser hybrid welding process were discussed. This alloy is characterized by high strength and is generally known as a material with good weldability. For the scientific evaluation of the microstructure, various characterization techniques have been used for the starting Al-alloy, in order to obtain the most realistic insight into the state of the microstructure and its properties.

2. Materials and methods

2.1. Used materials

The nominal chemical composition of Al-alloy AW 5454 is listed in Table 1.

Table 1. Chemical composition of alloy AW 5454 (in wt.%).

| Element | Si [%] | Fe [%] | Cu [%] | Mn [%] | Mg [%] | Cr [%] | Zn [%] | Ti [%] |
|---------|--------|--------|--------|--------|--------|--------|--------|--------|
| Minimum | - | - | - | 0.5 | 2.6 | 0.05 | - | - |
| Maximum | 0.25 | 0.4 | 0.1 | 1 | 3 | 0.2 | 0.2 | 0.05 |

Figure 2 shows a subassembly made of Al-alloy AW 5454, from which samples from the base sheet were targeted at selected locations for investigation. The shown sub-assembly is welded into the finished product in a further phase by laser hybrid welding of the Z-upper part and the S-lower part. For microstructure research, a sample on the

underside of the S beam from the E line was selected (the sample is marked SE). The thickness of the subassembly in this S part is 4 mm. Here, it should be emphasized that with more demanding forms of the Al-welded product, cracks occasionally appear in the central area along the weld, which is indicated in Figure 2 by the green area, due to clamping in the welding preparation.

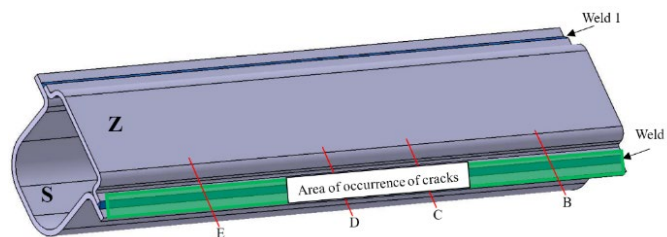


Fig. 2. Schematic representation of the demanding form of the sub-assembly from Al-alloy AW 5454 showing the lines B, C, D, and E that were chosen for research (Z- upper part, S- lower part); A green area where the probability of the appearance of cracks is very high.

2.1.1. Sample preparation

The SE sample preparation procedure followed classic metallographic preparation. The selected technological parameters for polishing are shown in Table 2.

Table 2. Technological parameters of polishing.

| Polishing agent | Load [N] | Rotational speed [rpm] | Direction of rotation | Time [min:s] |
|--------------------------------------|----------|------------------------|-----------------------|--------------|
| P600 sandpaper | 20 | 300/30 | Same direction | 5:00 |
| 9 μm diamond suspension + lubricant | 20 | 150/30 | Opposite direction | 5:00 |
| 3 μm diamond suspension + lubricant | 20 | 150/30 | Same direction | 4:00 |
| 1 μm diamond suspension + lubricant | 20 | 150/30 | Same direction | 2:30 |
| 0.06 μm colloidal silica + lubricant | 20 | 150/30 | Opposite direction | 2:00 |

After completion of the individual grinding/polishing steps, the sample was washed with running water. This was followed by cleaning in an ultrasonic bath in ethanol for 5 minutes and drying with dry air. After the final polishing with colloidal silica, the sample was cleaned in an ultrasonic bath for 20 min. This was followed by a process of chemical etching of the polished surface of the samples, which was carried out with an etchant (H₂O: HF = 10:1). Etching times varied from 10 s to several minutes.

2.2. Characterization methods

The microstructure of the selected sample was investigated with an optical metallographic microscope, NIKON Epiphot 300 (Japan), with an Olympus DP12 camera (Boston, USA). A Scanning Electron Microscope (SEM), Sirion 400NC (FEI, USA), with an Energy-Dispersive X-ray spectroscope INCA 350 (Oxford Instruments, UK), was used for detailed microstructure observation and microchemical analyses of the different metallic phases found in the sample. The sample was analyzed from secondary and backscattered electron images.

For better accuracy and to obtain as realistic an insight into the resulting microstructure as possible, a high-resolution field emission

electron microscope was used (Zeiss CrossBeam 550 FIBSEM) equipped with an EBSD camera (EDAX Hikari Super electron-backscatter diffraction) and EDS detector (EDAX Octane Elite energy-dispersive spectroscopy) and APEX software. This allowed for a variety of analyses, including secondary electron surface imaging, EDS, and EBSD analysis. For the investigations, a 15 kV accelerating voltage and a current of 2.0–5.0 nA were applied to the sensor for SE images. When performing the EBSD analysis, the sample was tilted at an angle of 70°, and the current on the sensor was 7.0 nA.

The hardness of the samples was examined with Vickers hardness measurements HV₅ on the ZWICK 3212 machine (Ulm, Germany). The measurement load of 5 kg was selected for the given sample dimensions. On the sub-assemblies S and Z, on lines B, C, and D (Fig. 2), the hardness measurements of HV₅ were carried out on the cross-sections, in such a way that the cut samples were metallographically prepared (ground and polished) following the procedure as shown in Table 2.

3. Results and discussion

3.1. Microstructure observation

The metallographic procedure was carried out according to the recommendations of BUEHLER SumMet („Buehler SumMet™ Metallography Techniques and Fundamentals Classes Offered in 2018“, 2018). During the metallographic preparation of the selected SE sample, problems arose during the preparation. After all stages of polishing, at the end of the preparation, numerous scratches and imprinted particles, originating from grinding and polishing agents, remained on the surface. Such an output polished microstructure is shown in Figure 3.

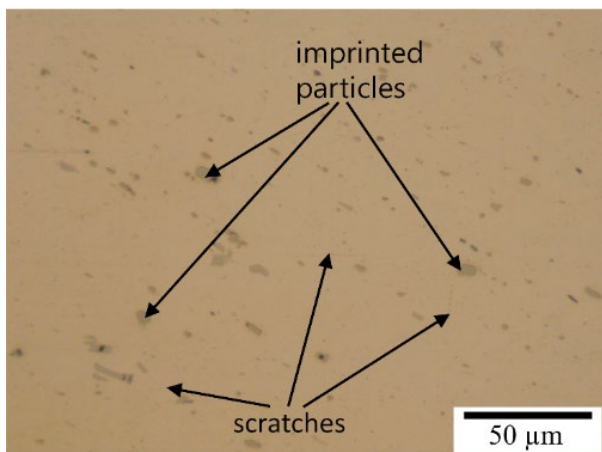
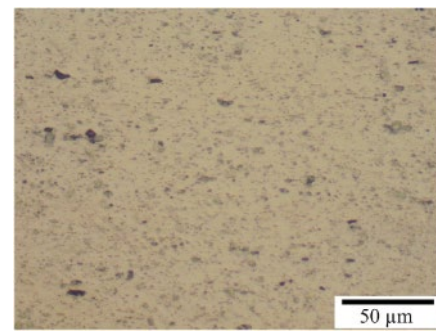


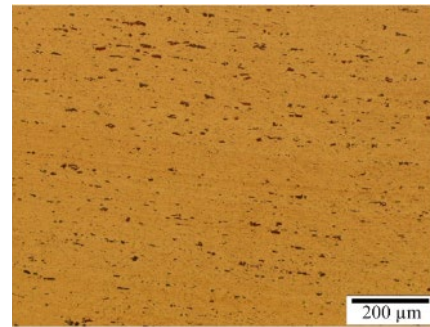
Fig. 3. Presentation of the optical microstructure of the polished surface of the SE sample.

With additional polishing, the resulting cracks did not significantly decrease, on the other hand, the number of imprinted particles from the polishing agent increased. Not-so-much better results were achieved using a lower pressure load when polishing, i.e. 20 N (instead of 25 N). Despite this, larger scratches and impressed particles from the polishing agent remained on the surface.

Chemical etching of the polished surface of the SE sample with an etchant (H₂O: HF = 10:1) in a time interval of 10 s and 60 s was not successful, as the initial microstructure was not detected. The findings were as follows: after 10 s, as well as, 60 s of etching, there is no significant change on the polished surface of the SE sample, which is shown in Figure 4.



a)



b)

Fig. 4. Presentation of the optical microstructure of the etched surface of the SE sample: a) t = 10 s; b) t = 60 s

In order to understand the resulting microstructure of the laser hybrid welded Al-alloy AW 5454, it is reasonable to analyze the changes in the microstructure and properties of the Al-alloy before welding and compare it after laser hybrid welding. During the metallographic preparation, we found that large microstructural changes occur already during the implementation itself, since the grinding and polishing processes of the surface of the samples result in the incorporation of abrasive agents (SiC, C, SiO₂ and Al₂O₃) into their surface. Based on this, detailed investigations on the polished surface of SE sample with a high-resolution line electron microscope with field emission of electrons was carried out (FEI Sirion 400 NC). We carried out point EDX microchemical analysis on the inclusions. Figure 5 shows the SEM microstructure of the SE sample with selected inclusions and spots for spot analysis. The results of EDX microchemical analyses at selected sites are shown in Table 3.

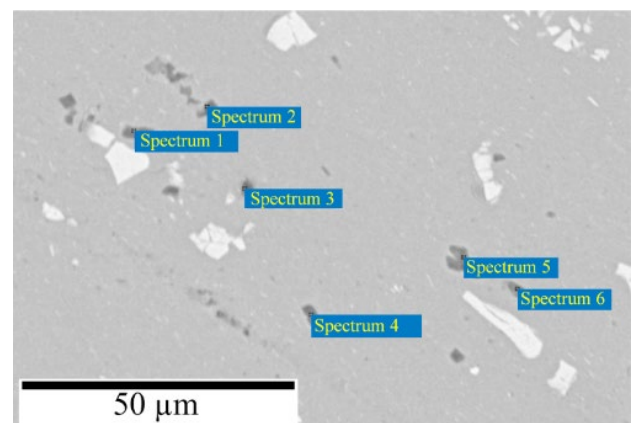


Fig. 5. SEM representation of the microstructure of the polished surface SE sample with selected sites for EDX microchemical analysis.

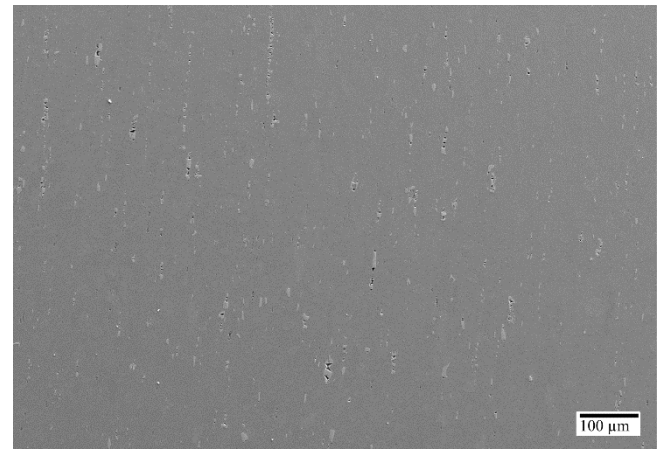
Table 3. Results of microchemical EDX analysis in wt. %.

| Spectrum | In stats. | C | O | Mg | Al | Si | Total |
|------------|-----------|-------|-------|-------|-------|-------|-------|
| Spectrum 1 | Yes | 6.76 | 31.11 | 5.57 | 33.65 | 22.91 | 100 |
| Spectrum 2 | Yes | - | 25.39 | 2.02 | 54.17 | 18.42 | 100 |
| Spectrum 3 | Yes | 81.52 | 2.55 | 0.50 | 15.05 | 0.37 | 100 |
| Spectrum 4 | Yes | 5.51 | 17.70 | 30.57 | 25.70 | 20.51 | 100 |
| Spectrum 5 | Yes | 8.32 | 24.02 | 3.62 | 48.80 | 15.24 | 100 |
| Spectrum 6 | Yes | 5.64 | 23.79 | 9.63 | 42.23 | 18.71 | 100 |

The results of the microchemical EDX analysis at the selected locations do not reflect the chemical composition of Al-alloy AW 5454 but indicate increased contents of Al, Si, O, C, and Mg, which are atypical elements for these Al-alloys. The elements are characteristic of abrasive/polishing agents that were otherwise used for the metallographic preparation of the surface of the SE sample. The quality of the surface preparation has a significant impact on the EDX microchemical analysis results, therefore it's important to keep an eye on everything that could alter the output microstructure, including inclusions, roughness, and cleanliness (Zupanič 1999). Based on an additional review of comparative literature (Sahoo, 2021; Slagter et al., 2024), it can be concluded that various inclusions (SiC , C, Al_2O_3) are present on the surface of the microstructure, which are typical representatives of abrasive agents, as they originate from the used grinding and polishing bases.

Based on the performed characterization and the obtained results of the EDS microchemical analysis, it was concluded that during the classic metallographic preparation of Al-alloy AW 5454, the imprinting of abrasive agents occurs. To acquire a more accurate understanding of the microstructure and, consequently, the characteristics of the investigated Al-alloy, an alternate technique of metallographic preparation was therefore pursued.

An analytical technique was used to prepare the microstructure of Al-metallographic samples, which included embedding the samples in a conductive bakelite resin, grinding and polishing the surface, and final treatment with an OPS (Oxide polishing suspension) suspension for 10 minutes. The characterization of the metallographically prepared surface was performed using a high-resolution field emission electron microscope (Zeiss CrossBeam 550 FIBSEM). Figure 6 shows the exposed SEM microstructure of the SE sample. Upon careful examination, no abrasives or polishing agents were found.

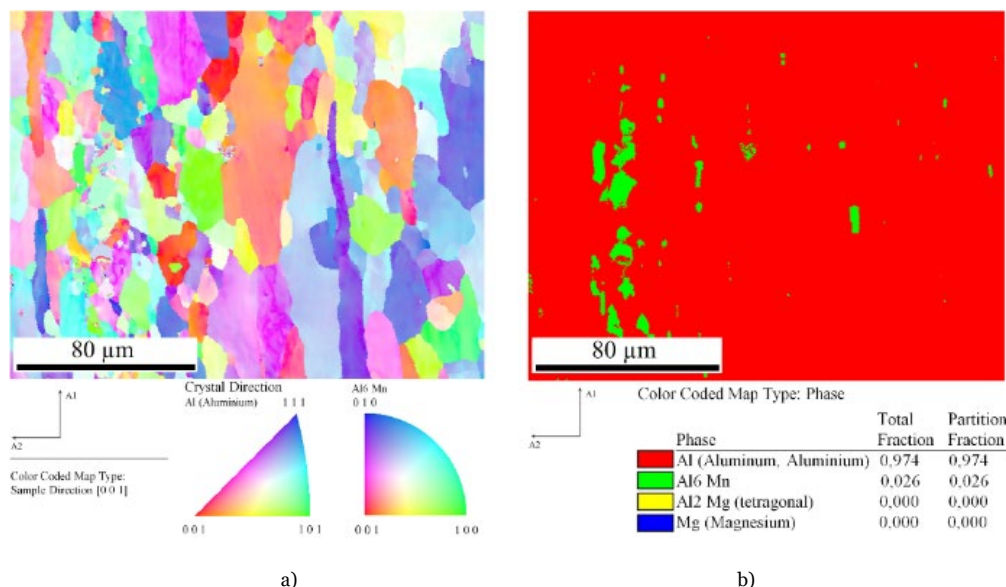
**Fig. 6.** SEM microstructure of SE sample.

This was followed by the performance of EBSD analysis on the same surface of the selected SE sample, where it was discovered that the main phase in the alloy is α -aluminum, in which Mg and Si are dissolved (Figure 7a). The presence of a very fine Mg_2Si phase was also identified, the surface fraction of which is below 1 %, which is within the margin of error. Therefore, EDX mapping was additionally performed, which confirmed the presence of both elements of the Mg_2Si phase and thus the existence of the phase itself (Figure 7b). The main phase of $\text{Al}_6(\text{Mn}, \text{Fe})$ was also identified in a surface proportion between 1.2 and 2.6 %.

The results of the analyzed phases will serve as a basis for further research and understanding of the discussed problem of crack formation in laser hybrid welds on Al-alloy AW 5454.

3.2. Hardness

On selected samples of S and Z subassemblies, the microhardness HV₅ was measured on metallographically prepared cross-sections (Broitman, 2016). Figure 8 shows an example obtained for selected samples, while the results of all HV₅ measurements on the samples are recorded in Table 4.

**Fig 7.** a) EBSD analysis of the microstructure of SE sample and b) EDX mapping for the Mg_2Si phase.

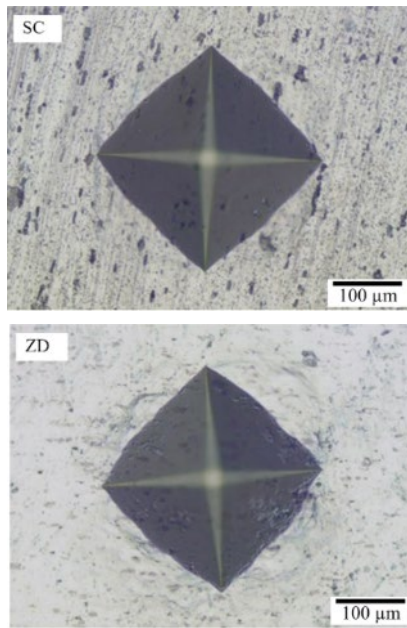


Fig. 8. HV5 impression on the sample: a) SC and b) ZD sample.

Table 4. The average of the HV5 hardness measurements on the cross-sections of samples S and Z.

| Sample | No. of measurements | Average sample hardness | Std. deviation |
|--------|---------------------|-------------------------|----------------|
| S C | 14 | 81.4 | 5.9 |
| S D | 13 | 84.0 | 5.1 |
| S E | 10 | 85.2 | 3.3 |
| Z B | 12 | 87.6 | 5.6 |
| Z D | 16 | 85.9 | 5.9 |
| Z D | 16 | 88.5 | 5.9 |

Table 5. Average of HV5 hardness measurements on S and Z samples.

| Sample | No. of measurements | Average sample hardness | Std. deviation |
|--------|---------------------|-------------------------|----------------|
| S | 37 | 83.3 | 5.3 |
| Z | 44 | 87.3 | 5.9 |

From the HV5 results shown in Figure 4 and 5, it can be seen that the HV5 average value on the thicker sample S (4 mm) and the thinner sample Z (3.5 mm) differs by approximately 5 %, which indicates the probable strengthening of the Al-alloy due to rolling process and subsequent cold forming (Conserva, Donzelli, and Trippodo, 1992; Davis, 2001). It is known that AW 5454 alloy can only be hardened by kneading. The hardening of this alloy does not affect its properties during subsequent welding, as the Al-alloy softens in the vicinity of the weld joint, thus regaining its properties before processing (Conserva, Donzelli, and Trippodo, 1992; Davis, 2001).

4. Conclusions

In the first part, laser surface modification techniques were presented, where the development goes in the direction of abandoning dust melts and intending to introduce laser hybrid welding. This applies especially to Al-alloys, where it is necessary to know the initial microstructure and their hardness.

Microstructural investigations of Al-alloy AW 5454 revealed that the metallographic preparation is very demanding. This results in the imprinting of various abrasive/polishing agents, which cannot be removed during subsequent preparation. For this, it is necessary to undertake a unique preparation with an OPS suspension, which

allows obtaining a polished surface without inclusions. The revealed microstructure is practically single-phase as α -aluminum with more than 97.4 surface area, and $Al_6(Mn, Fe)$ and Mg_2Si phases are also present. The results of HV5 indicate that the Al-alloy surface is different in hardness, depending on the conditions of previous mechanical processing and clamping.

Based on this study, it will be necessary to take into account all discovered facts in the process of laser hybrid welding and to consider them when changing the Al-alloy microstructure, which will be the result of welding.

References

- Abeens, M., R. Muruganandhan, K. Thirumavalavan, and S. Kalainathan. "Surface Modification of AA7075 T651 by Laser Shock Peening to Improve the Wear Characteristics." *Materials Research Express* 6, no. 6 (2019): 66519-32.
- Biswas, Sourabh. "Laser Surface Melting of Carbon Coated AA7075 Aluminum Alloy: Structural Transformations and Tribological Behavior." ProQuest Dissertations Publishing, 2014.
- Broitman, Esteban. "Indentation Hardness Measurements at Macro-, Micro-, and Nanoscale: A Critical Overview." *Tribology Letters* 65, no. 1 (2016): 23.
- Buehler, "Buehler SumMet™ Metallography Techniques and Fundamentals Classes Offered in 2018." PRWeb Newswire, 2018.
- Cavaliere, Pasquale. *Laser Cladding of Metals*. Springer International Publishing, 2021.
- Chen, Chao, Xinyue Cong, Jiuqing Liu, and Huijing Zhang. "Influences of Heat Input on the Geometric Parameters and Element Distribution of CrMnFeCoNi High-Entropy Alloy Coating on Aluminum Alloy Using Laser Cladding." *Transactions of the Indian Institute of Metals* 76, no. 5 (2023): 1271-80.
- Conserva, M., G. Donzelli, and R. Trippodo. *Aluminium and Its Applications*. Edimet, 1992.
- Dai, Hongjie. "Carbon nanotubes: opportunities and challenges." *Surface Science* 500, no. 1 (2002): 218-41.
- Davis, J. R. *Aluminum and Aluminum Alloys. V Alloying - Understanding the Basics*. 2nd ed. ASM International, 2001.
- Eatemadi, Ali, Hadis Daraee, Hamzeh Karimkhanloo, Mohammad Kouhi, Nosratollah Zarghami, Abolfazl Akbarzadeh, Mozhgan Abasi, Younes Hanifehpour, and Sang Woo Joo. "Carbon nanotubes: properties, synthesis, purification, and medical applications." *Nanoscale Research Letters* 9, no. 1 (2014): 393.
- Fribourg, G., A. Deschamps, Y. Bréchet, G. Mylonas, G. Labeas, U. Heckenberger, and M. Perez. "Microstructure Modifications Induced by a Laser Surface Treatment in an AA7449 Aluminium Alloy." *Materials Science & Engineering: A* 528, no. 6 (2011): 2736-47.
- He, Zhaoru, Yizhou Shen, Jie Tao, Haifeng Chen, Xiaofei Zeng, Xin Huang, and Ali Abd El-Aty. "Laser Shock Peening Regulating Aluminum Alloy Surface Residual Stresses for Enhancing the Mechanical Properties: Roles of Shock Number and Energy." *Surface & Coatings Technology* 421 (2021).
- Jin, Yajuan, Baochun Lu, and Xudong Tang. "Crack-Free Copper Alloy Coating on Aluminum Alloy Fabricated by Laser Cladding." *Coatings* 13, no. 9 (2023): 1491.
- Kandavalli, Sumanth Ratna, Gadudasu Babu Rao, Praveen Kumar Banaravuri, Manu Mathai Kanakamani Rajam, Sunanda Ratna Kandavalli, and S. Rajesh Ruban. "Surface strengthening of aluminium alloys/composites by laser applications: A comprehensive review." *Materials Today: Proceedings* 47 (2021): 6919-25.
- Liu, Quanbing, Zongde Liu, Yue Shen, Yanru Chang, Jiaxuan Li, and Yi Xiao. "A Method for Preparing Alloy Coating on the Aluminum Alloy Substrate via Laser Cladding Technology to Prevent the Galvanic Corrosion of TC4/5083 Couple." *Materials Letters* 357 (2024).
- Lu, Liang, Ting Huang, and Minlin Zhong. "WC Nano-Particle Surface Injection via Laser Shock Peening onto 5A06 Aluminum Alloy." *Surface & Coatings Technology* 206, no. 22 (2012): 4525-30.
- Luo, Kaiyu, Yu Xing, Muran Sun, Lujie Xu, Shengkai Xu, Changyu Wang, and Jinzhong Lu. "Effect of Laser Shock Peening on the Dissolution of Precipitates and Pitting Corrosion of AA6061-T6 with Different Original Surface Roughness." *Corrosion Science* 228 (2024).
- Nayak, Subhadarshi. "Laser Induced Surface Modification of Aluminium Alloys." University of Tennessee - Knoxville, 2004.
- Raabe, Dierk, Dirk Ponge, Peter J. Uggowitzer, Moritz Roscher, Mario Paolantonio, Chuanlai Liu, and Helmut Antrekowitsch. "Making sustainable aluminum by recycling scrap: The science of "dirty" alloys." *Progress in Materials Science* 128 (2022): 100947.
- Renk, Karl F. *Basics of Laser Physics. For Students of Science and Engineering*. 1st ed. Springer Nature, 2012.
- Sahoo, Sarmila. "Aluminium Hybrid Composites Reinforced with SiC and Fly Ash Particles—Recent Developments." In *Recent Advances in Layered Materials and Structures*, 133-70. Springer Singapore Pte. Limited, 2021.
- Saklakoglu, Nursen, Simge Gencalp Irizalp, Erhan Akman, and Arif Demir. "Near surface modification of aluminum alloy induced by laser shock processing." *Optics & Laser Technology* 64 (2014): 235-41.

Simon, Juliette, Emmanuel Flahaut, and Muriel Golzio. "Overview of Carbon Nanotubes for Biomedical Applications." *Materials* 12, no. 4 (2019): 624.

Slagter, Alejandra, Jonathan Aristya Setyadi, Eva Luisa Vogt, David Hernández-Escobar, Léa Deillon, and Andreas Mortensen. "Nanoindentation Hardness and Modulus of Al₂O₃-SiO₂-CaO and MnO-SiO₂-FeO Inclusions in Iron." *Metallurgical and Materials Transactions A* 55, no. 5 (2024): 1469-83.

Sui, Qi, Ning Hu, Yingrui Su, Yan Wang, and Xiaolei Song. "Tensile Property of 7075 Aluminum Alloy with Strengthening Layer by Laser Remelting-Cladding Treatment." *Micromachines* 14, no. 11 (2023): 2017.

Trdan, U., J.L. Ocaña, and J. Grum. "Surface modification of aluminium alloys with Laser Shock Processing." *STROJNISKI VESTNIK-JOURNAL OF MECHANICAL ENGINEERING* 57, no. 5 (2011): 385-93.

Tsagkarakis, M.G., F.J. Villarreal, H.J. Baker, D.R. Hall, and S.W. Williams. "Surface Melting of Al-Cu-Mg Alloy Using a Short-Pulse, Planar Waveguide CO₂ Laser for Corrosion Resistance Improvement." *Journal of Laser Applications* 15, no. 4 (2003): 233-39.

Watkins, K.G., M.A. McMahon, and W.M. Steen. "Microstructure and Corrosion Properties of Laser Surface Processed Aluminium Alloys: A Review." *Materials Science & Engineering: A* 231, no. 1 (1997): 55-61.

Zhao, Pengfei, Zimu Shi, Xingfu Wang, Yanzhou Li, Zhanyi Cao, Modi Zhao, and Juhua Liang. "A Review of the Laser Cladding of Metal-Based Alloys, Ceramic-Reinforced Composites, Amorphous Alloys, and High-Entropy Alloys on Aluminum Alloys." *Lubricants* 11, no. 11 (2023): 482.

Zupanič, Franc, and Ivan Anžel. *Gradiva*. Maribor: Fakulteta za strojništvo, 2007.

Zupanič, Franc. *Gradiva: praktikum*, 1st ed. Maribor, 1999.